Jammed Emulsions with Adhesive Pea Protein Particles for Elastoplastic Edible 3D Printed Materials

Simha Sridharan, Marcel B. J. Meinders, Leonard M. Sagis, Johannes H. Bitter, and Constantinos V. Nikiforidis*

3D printed materials are of great relevance to produce medicinal scaffolds and specialized foods. An approach to forming 3D printable materials is to use jammed oil droplets. Jammed oil droplets are highly viscous and can be extruded through the nozzle of a 3D printer, while after chemical cross-linking they acquire a self-standing ability. However, the molecules currently used to stabilize and cross-link the oil droplets have questionable biocompatibility. Therefore, this study aims to produce a 3D printable jammed emulsion using pea proteins. This jammed oil-in-water emulsion is remarkably stable and viscoelastic enough to be extruded through the printer nozzle. Adhesive pea protein particles formed by pH adjustment act as physical cross-links between the oil droplets, forming a scaffold with elastoplastic rheological properties that flows above critical stress while, without any additional treatment, exhibits the required self-standing properties for 3D printing. By understanding the properties of pea proteins and their behavior in bulk and on interfaces, pea protein-based 3D printable material is created for the first time.

1. Introduction

Manufacturing materials using 3D printing is simple, yet effective in creating intricate macroscopic structures.[1,2] 3D printing technique involves, pushing the material through a nozzle and depositing it layer-by-layer to produce the required structure.[2,3] The challenge is to create a material that flows when stress is applied to pass through the nozzle, while it behaves as solid at rest to hold the printed structure.[4] Materials with such rheological properties are known as plastic or yield stress materials.

The applications of 3D printing range from scaffolds for tissue cartilages and specialized functional foods.[3,5–7] Currently food printing is mostly performed using carbohydrate polymer materials, with added cross-linking agents and other natural fillers such as vegetables or chocolates.[8,9] Besides 3D printing conventional foods with attractive designs, 3D printing is also widely studied to create specific food structures for specialized nutrition. For instance, 3D printing is investigated to produce foods for elderly with mastication issues.[10] 3D printing can also be used to make foods with specific composition in the context of personalized nutrition.[11–13]

Unlike 3D printing traditional foods, specialized foods need to meet specific microstructure and nutrient requirements. This demands creation of materials with precisely controlled composition and rheological properties. However, the number of edible biopolymers that can be used to create food materials that possess the necessary plastic properties for 3D printing is extremely limited.[14]

A route for creating edible 3D materials is the use of highly concentrated oil-in-water emulsions. The examples reported in the literature are concentrated oil-in-water emulsions with an oil volume fraction φ larger than 0.64, and with the oil droplets stabilized through a Pickering mechanism by crystalline biobased particles such as chitin or cellulose nanocrystals.[1,5,7,15] The crystalline particles at the droplet interface and also in the continuous phase create droplet–droplet interaction through weak physical attractive forces resulting in a soft elastic material, which can flow when subjected to sufficiently large shear stresses. However, to provide a self-standing property after flowing, chemical cross-linking and thermal treatments of the material are often necessary.[5] This step, together with the production step of the crystalline particles used as stabilizers, often reduces the biocompatibility of the materials their potential use in foods.

Therefore, there is a need for printable emulsions where commonly accessible and edible polymers are used as stabilizing and cross-linking agents. An attractive edible biopolymer source

S. Sridharan, Prof. J. H. Bitter, Dr. C. V. Nikiforidis
Laboratory of Bio-based Chemistry and Technology (BCT)
Wageningen University
P. O. Box: 17, Bornse Weilanden 9, Wageningen 6708 WG, The Netherlands
E-mail: costas.nikiforidis@wur.nl
S. Sridharan, Dr. M. B. J. Meinders
TiFN
Nieuwe Kanaal 9A, Wageningen 6709 PA, The Netherlands
Dr. M. B. J. Meinders
Wageningen Food and Bio-based Research (FBR)
Wageningen University and Research Centre
P. O. Box: 17, Bornse Weilanden 9, Wageningen 6708 WG, The Netherlands
Dr. L. M. Sagis
Laboratory of Physics and Physical Chemistry of Foods
Wageningen University
Bornse Weilanden 9, Wageningen 6708 WG, The Netherlands

**ADVANCED
SCIENCE NEWS**

www.advancedsciencenews.com

**ADVANCED
FUNCTIONAL
MATERIALS**

www.afm-journal.de

that has not been used before to design emulsions that can be printable is plant-based proteins such as pea proteins.

Pea proteins have gained wide attention due to the lower environmental impact associated with them.[16] Moreover, pea proteins have excellent emulsifying properties and are widely available for use in edible applications.[17–20] Pea proteins assemble through physical attractive forces into adhesive protein particles at pH 3,[21] which could act as natural cross-linking agents.[5]

In this work, we investigated the oscillatory rheological properties of jammed emulsions stabilized by pea proteins and linked them to 3D printability. We established the role of the pea protein particles formed by pH triggered self-assembly, in creating printable edible emulsions. Our research reveals that due to the adhesive properties of the pea protein particles the droplets within the jammed emulsions are "glued" together enabling the formation of 3D printable edible materials. We present a simple pH driven approach to create edible materials with 3D printable properties using pea proteins without the aid of additional cross-linking agents.

2. Results and Discussions

2.1. Microstructure and Rheological Properties of Jammed Emulsions Stabilized by Pea Protein Molecules

To be relevant to edible and biocompatible applications, we extracted pea proteins following a simple procedure.[17,21,22] The obtained pea proteins exist predominantly as individual protein molecules with a ς-potential of about −25 mV at pH 7.[21,23,24] These protein molecules (pH 7) were used (1.4 wt%) to stabilize jammed oil-in-water emulsions containing 70 wt% oil ($\varphi = 0.72$).[25]

The oil droplet size distribution of the emulsions is shown in **Figure 1**a. The size distribution was monomodal with droplets mostly between 1 and 10 µm. The distribution in droplet sizes and the deformable nature of the oil droplets enable their packing above the theoretical random close packing fraction ($\varphi = 0.64$) in these emulsions. It shows that pea proteins can stabilize emulsions well above the oil droplet packing volume fraction ($\varphi = 0.64$), indicating their excellent emulsifying ability. The microstructural properties of the jammed oil droplets were

investigated using confocal microscopy (Figure 1b). The image shows oil in red and proteins in green. The images show that pea proteins can stabilize oil droplets in close contact with each other.

For the emulsions to be 3D printed, they should possess a strong yield stress behavior (plastic). Therefore, to characterize whether the formed jammed emulsion is suitable for 3D printing, the rheological properties were investigated. The rheological shear elastic (G′) and loss modulus (G″) of the emulsions as a function of frequency (0.1–100 rad s^{-1}) at constant strain (0.5%) and as a function of strain amplitude (0.1–1000%) at a constant frequency of 6.28 rad s^{-1} are shown in **Figure 2**a,b.

The frequency-dependent response provides insights in the dynamics of microstructural changes during shear (Figure 2a). The G′ of the pea protein stabilized emulsions was higher than G″ over the entire range of applied frequencies. The elastic nature of the emulsions results from the Laplace pressure of the jammed droplets. Moreover, the elastic and loss moduli have a power law dependence on frequency, suggesting that the material behaves like a viscoelastic soft solid.[26,27]
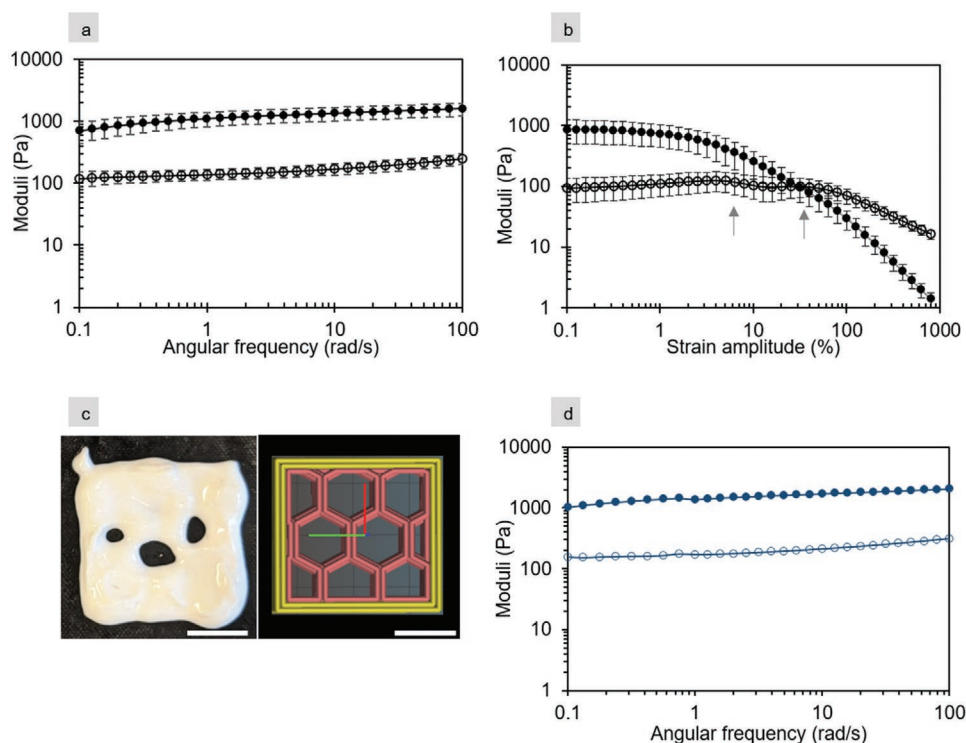
Figure 2b shows the G′ and G″ curves as a function of strain amplitude in a log–log plot. The rheological response of the emulsions as a function of strain provides information on structure breakdown and whether it possesses a plastic-like rheological response necessary for 3D printing. The elastic moduli (G′) were higher than the loss moduli (G″) at low and intermediate strains (strain amplitude < 20%), indicating the emulsions behave predominantly as an elastic material.

The G′ curve as a function of strain decreases gradually above 2% strain progressively until about 40% strain. From a strain amplitude of about 40%, G′ is smaller than G″ and the system behaves more as a viscoelastic liquid. The gradual decrease in G′ shows that the microstructure breakdown was smooth, probably due to gradual loss of droplet–droplet contact as strain increases.

The loss moduli (G″) curves as a function of strain in Figure 1c reveal additional information about the microstructure of the jammed emulsions. The G″ curve shows two strain values where G″ first mildly increases, followed by a decrease, which is called a weak overshoot.[28] This is attributed to the
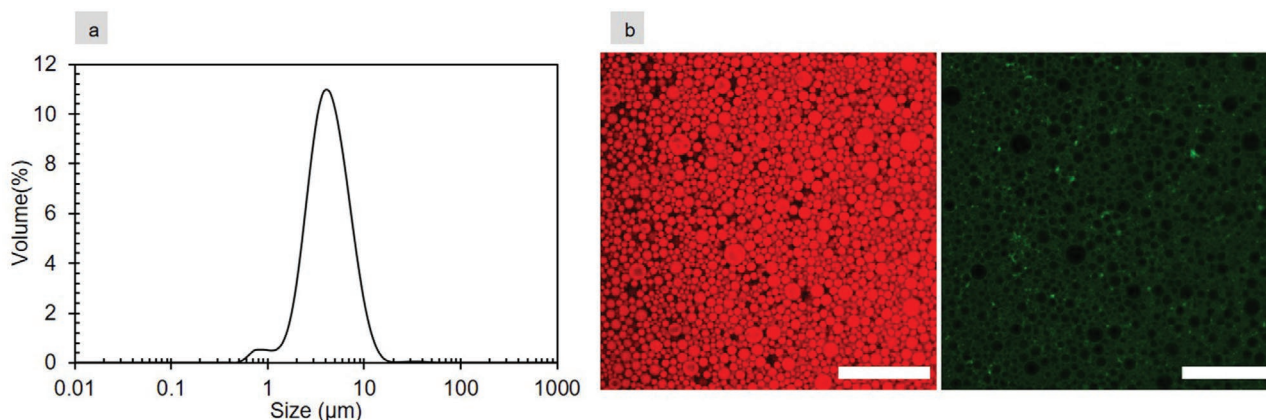
Figure 1. a) Oil droplet size distribution of 70.0 wt% oil-in-water emulsions at pH 7 stabilized with 1.4 wt% pea proteins. b) Confocal image of emulsion stabilized with pea protein molecules. Oil in red (Nile red) and protein in green (Fast Green), scale bar: 50 µm.

ADVANCED
SCIENCE NEWS
www.advancedsciencenews.com

ADVANCED
FUNCTIONAL
MATERIALS
www.afm-journal.de

Figure 2. Elastic (G″: filled symbols) and loss modulus (G″: open symbols) of 70 wt% oil emulsion stabilized by pea protein molecules as a function of a) increasing frequency at a constant strain of 0.5% and b) as a function of increasing strain at a constant frequency of 6.28 rad s^{-1}. c) Photographs of pea protein stabilized emulsion upon 3D printing at room temperature, top view with scale bar 1 cm and the envisioned honeycomb structure: 3 cm * 3 cm * 1 cm ($l*w*h$). d) Elastic (G′: filled symbols) and loss modulus (G″: unfilled symbols) as a function of frequency for 3D printed emulsion (a flat dense cylinder of diameter of 5 cm and height of 2.5 mm).

typical behavior of highly concentrated emulsions and jammed systems.[29–31] The overshoot arises when sudden flow or rearrangement occurs within jammed emulsions. Initially, under small strains, the jammed emulsions droplets are restricted to move due to the neighboring droplets. However, as strain increases, the droplets break their confinement momentarily and start to flow or rearrange.

The first overshoot occurs around 5% strain and the second around 40% strain and these may be related to two different microstructural relaxation processes.[32] The first overshoot at low strain could be related to the disruption of droplet contact. Even though the droplet contacts are broken, due to the high concentration of droplets, they cannot yet move and are trapped in a cage of surrounding droplets.[33] The second overshoot (G″) at a higher strain (≈40%) is related to large droplet rearrangement or flow. At this higher strain, droplets escape their cage, and the emulsion starts to flow.[32,34] Therefore, the emulsions exhibited a typical rheological response of a jammed emulsion system, with only weak droplet–droplet interactions.[35,36]

The jammed emulsion stabilized by pea protein molecules was tested for their 3D printability using extrusion-based 3D printing at room temperature. The emulsions were extruded with a continuous flow through the nozzle having a pore size of 1200 μm. However, after printing a honeycomb structure ($l*w*h$ = 3 cm * 3 cm * 1 cm) with 13 layers, the emulsions were not able to self-support their structure (Figure 1d). The emulsion structure collapsed within a few minutes and the different

layers merged. Even though the emulsions were jammed and have viscoelastic soft solid properties, the G′ and G″ were not sufficient to retain the printed structure. This is likely due to insufficient droplet–droplet attractive forces.

For 3D printing, a nozzle with large pore size of 1200 μm was used. Such a large nozzle dimension provides the ability to easily extrude our material and deposit it onto the surface. Moreover, droplet sizes in the emulsions are mostly below 10 μm, therefore flow through the nozzle is not expected to destabilize the oil droplets. No oiling off was observed, indicating that the emulsion droplets did not destabilize.

To test the effect of 3D printing on the material property, a frequency sweep on the emulsions was performed after 3D printing. For this purpose, a cylindrical shape was printed instead of a honeycomb (see the Experimental Section). Figure 2d shows frequency sweep after 3D printing. The figure shows that even after 3D printing G′ is higher than G″ following the same pattern as before 3D printing (Figure 4a). This finding clearly shows that the material properties are unaffected by 3D printing.

2.2. Moving from Soft Jammed to Plastic Emulsion Material Using Adhesive Pea Protein Particles

To increase droplet–droplet interaction for 3D printing of emulsions, cross-linking and/or thermal treatments are commonly

employed.[3,5] However, for edible applications, it is desirable to avoid such chemical cross-linking, therefore we attempted to use the adhesive nature of pea protein particles to create stronger droplet–droplet interactions by changing the pH of the protein dispersion before emulsification.

Pea proteins, upon pH change to pH 3 in an aqueous phase, self-assemble into protein particles with sizes between 50 and 500 nm. This is despite that; they possess a surface charge of about +30 mV.[21,37] The protein particles are formed through attractive hydrophobic and van der Waals forces that overcome the electrostatic repulsion.[21] The dispersed pea protein particles under these conditions are in equilibrium with single protein molecules at a weight ratio of 60:40. As shown by emulsification and interfacial measurements, when a mixture of pea protein particles and molecules are used to stabilize oil droplets, the protein molecules are mainly adsorbed on the oil droplet interface. The protein molecules are sufficient to produce stable emulsion droplets of the same size as when they are mixed with protein particles. These protein particles do not take part in interfacial stabilization, but simply adhere to the primary protein layer on the oil/water interface, or are present in the bulk.[21] Due to the attractive nature of protein particles, they could "glue" neighboring oil droplets when they are forced to be in contact, like in a jammed emulsion (see Figure 7b).

To investigate the potential use of the pea protein particles for this purpose, we triggered the formation of particles by adjusting the pH of a protein dispersion to pH 3 before forming jammed emulsions (70 wt% oil, $\varphi = 0.72$). At this condition, pea protein molecules are expected to be adsorbed on the interface, while the protein particles are expected to be entrapped between the oil droplets.

Figure 3 shows the oil droplet size distribution for emulsions at pH 3 and the confocal image of the emulsions. The droplet size of the formed emulsions was again monomodal and droplets were mostly between 1 and 10 µm. Pea proteins form similar droplet size at both pH 7 and pH 3.

The microstructure of emulsions in the presence of protein particles (Figure 3b), as observed with confocal microscopy, shows that the droplets are closely packed. Protein particles (green fluorescence) are clearly visible between the packed oil droplets. These were not seen when only pea protein molecules were used to stabilize the emulsions.

Regarding the rheological properties of the jammed emulsions with pea protein particles, the elastic and loss modulus as a function of frequency is shown in **Figure 4**a. The emulsions showed higher G′ than G″ with both depending on frequency as a power law, showing that they behave as soft solids, similar to when only pea protein molecules were used (Figure 2a). However, the absolute values of the elastic and loss modulus of emulsions with pea protein particles were higher than the emulsion where only pea protein molecules were present. This points to a stronger droplet–droplet interaction when protein particles are present.

The elastic and loss moduli of the emulsions in the presence of protein particles as a function of strain are shown in Figure 4b. At low strains, the G′ curve is higher than G″ indicating a predominantly elastic behavior. Unlike emulsions with only pea protein molecules, there is no gradual decline, but a sharp decrease in G′ occurs above 10% strain. At strain around 15%, the G′ curve crosses the G″, indicating a predominantly

viscous response for strain amplitudes larger than about 15%. The decrease in G′ is related to the breakdown of the microstructure, due to loss of contact between neighboring droplets. In these systems, the yielding of the structure is much more abrupt than in the jammed emulsions stabilized by protein molecules.

The loss moduli curve shows a single sharp overshoot at the same time the G′ drops, demonstrating a sharp loss of droplet–droplet contact and immediate flow or rearrangement.[38,39] The sharp structural change points to the presence of strong droplet–droplet interactions and network formation. In such systems the process of bond breaking, and cage disruption occur simultaneously, leading to a single overshoot. Pea proteins associate with protein particles through physical forces such as van der Waals and hydrophobic forces that overcome the weak electrostatic forces at pH 3. The electrostatic forces are not strong enough to prevent the association of pea proteins at this condition.[13] Similarly, the droplet–droplet network could be mediated by protein particles through attractive hydrophobic and van der Waals forces.

The disruption in interaction due to strain leads to the flow of the material, which is desirable for pushing the emulsion through the nozzle for 3D printing. Besides, due to the higher stiffness at low strains, the material can be expected to retain its shape better upon depositing from the nozzle. Therefore, the emulsion may be a suitable candidate for 3D printing through a simple extrusion method.

The emulsions with pea protein particles were tested for their printability by extrusion-based additive manufacturing a honeycomb structure. The emulsions flowed through the nozzle (1200 µm pore size) in a continuous manner. The photographs of the printed structures are shown in Figure 4c. The emulsions were able to retain the printed structure as seen from the photographs. The shape of the extruded material was also clearly visible and resulted in a sharp printed structure. The cross-section (Figure 4c) shows that the emulsion layers deposited by the 3D printer were distinct and self-supported.
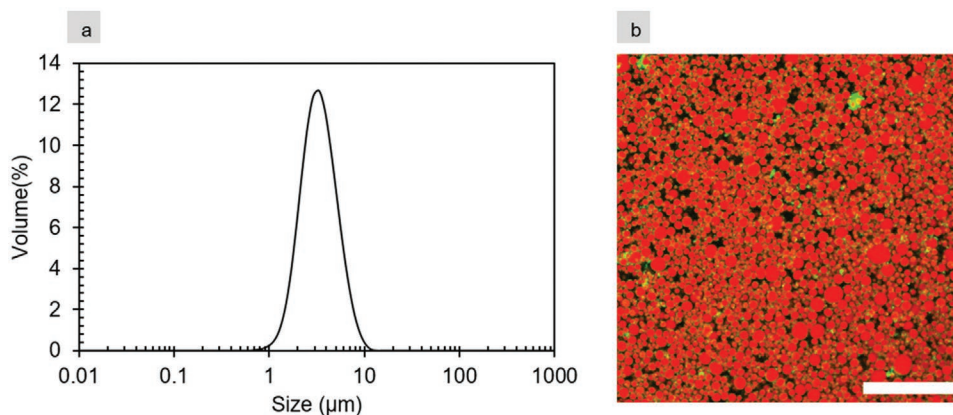
The self-supporting structure retained its shape for over 48 h (Figure 4d) without the need for any postprinting treatment. During this period, there was no oiling off of the printed structure, indicating that the emulsions were not destabilized.

The rheological behavior of the emulsions was also tested after 3D printing using a frequency sweep. The frequency sweep is shown in Figure 4e. The figure shows that G′ is higher than G″ following the same pattern as the emulsion before 3D printing (Figure 4a). This similar behavior shows that, 3D printing does not affect the material properties.

We successfully designed a 3D printable material by using jammed emulsion in the presence of pea protein particles. The stability of the printed structure clearly shows that, without any additional treatments, like chemical cross-linking, adhesive pea protein particles can enhance the interactions between neighboring oil droplets through hydrophobic and van der Waals forces.

2.3. Pea Protein Particles Stick Jammed Oil Droplets Together through Physical Forces

To get more direct insights into the role of the protein particles, we analyzed the nonlinear shear rheology of the emulsions

**ADVANCED
SCIENCE NEWS**

www.advancedsciencenews.com

**ADVANCED
FUNCTIONAL
MATERIALS**

www.afm-journal.de

Figure 3. a) Oil droplet size distribution of 70.0 wt% oil-in-water emulsions at pH 3 stabilized with 1.4 wt% pea proteins. b) Confocal image of emulsion stabilized with pea protein molecules. Oil in red (Nile red) and protein in green (Fast Green), scale bar: 50 μm.
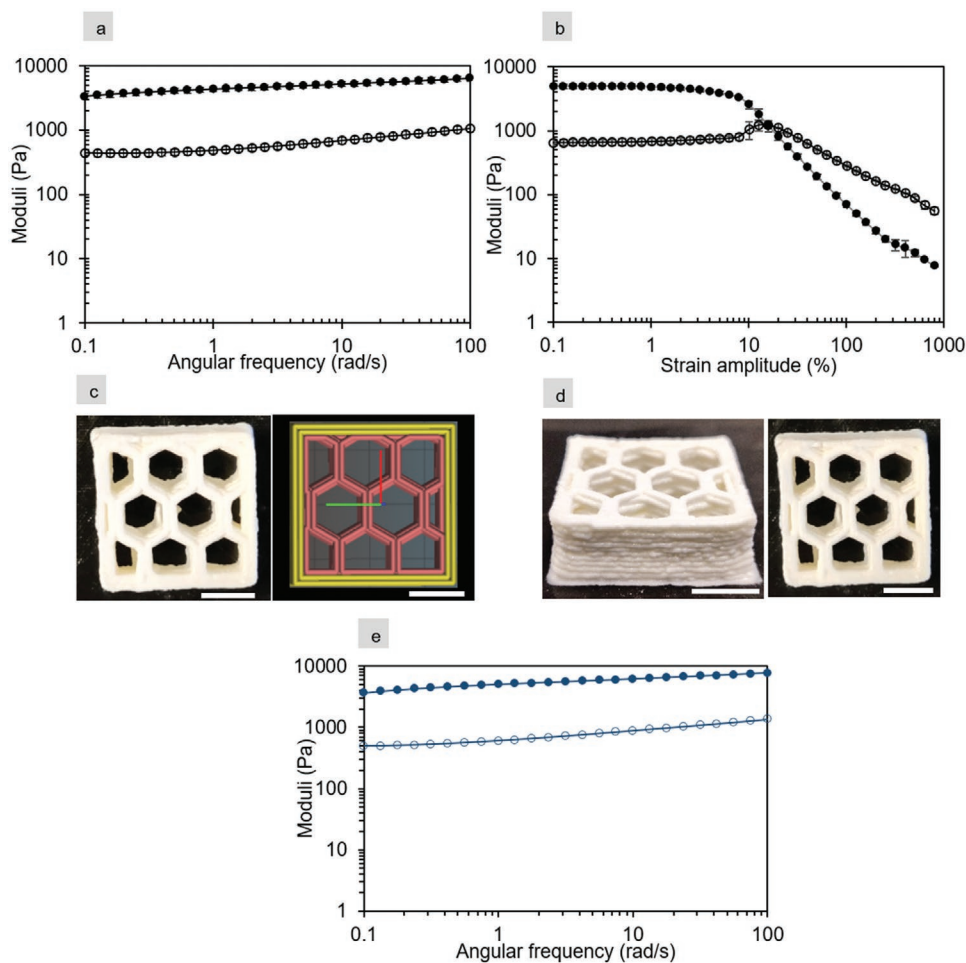
Figure 4. a) Elastic (G″: filled symbols) and loss modulus (G″: unfilled symbols) as a function of increasing frequency at a constant strain of 0.5% and b) as a function of increasing strain at a constant frequency of 6.28 rad s^{-1}. c) Photographs of 3D printed emulsions in the presence of protein particles at room temperature top view with scale bar: 1 cm with print dimensions of 3 cm * 3 cm * 1 cm (*l*w*h*) and the designed honeycomb structure to be 3D printed and d) 3D printed structure after 48 h of storage at room temperature. e) Elastic (G′: filled symbols) and loss modulus (G″: unfilled symbols) as a function of frequency for 3D printed emulsion (a flat dense cylinder of diameter of 5 cm and height of 2.5 mm).

using Lissajous plots (more information about these plots is in the Supporting Information). These plots provide a way to investigate further the breakdown of the microstructure and provide a rheological fingerprint of the material properties. For instance, for a material to be 3D printable, a plastic material response is required. For such a material the Lissajous plots take on a rectangular shape (**Figure 5**a). Therefore, to assess 3D printability of materials, characterizing their Lissajous plots against standard curves would be a powerful approach.

Lissajous plots were plotted for jammed concentrated emulsions both with and without pea protein particles (Figure 3). The figures show a loop plotted as total stress versus total strain normalized by the maximum stress and strain, respectively. A dashed line inside the loop is also plotted, which corresponds to the elastic contribution to the total stress.[40]

At low strains (10.1%), emulsions without protein particles show a tilted nearly elliptical shape closely resembling the reference curve in Figure 5a. This shape points to a mildly non-linear viscoelastic behavior, which was in-line with the G' and G'' measurement of the amplitude sweep.[41] The elastic contribution to the stress showed a nearly straight line, with a slight increase in slope near the maximum strain, which points to a weak strain hardening behavior. By contrast, at 10.1% strain, emulsions with protein particles show a more rhomboidal shape, with intracycle softening behavior near the maximum strain.

At 50% and 100% strain, emulsions without protein particles show wider loops in the form of a rounded rhomboid. The increase in loop area at these strains demonstrates that the viscous component becomes more apparent compared to the elastic component.[41] The shape of these plots corresponds to emulsions which show progressive softening upon increased strain while maintaining a small but finite slope in the elastic contribution. This is consistent with our earlier observation

that there is no abrupt yielding in these systems, and that for emulsions without protein particles, the droplet–droplet interactions are relatively weak.

Contrarily, at 50% and 100% strains, emulsions with protein particles show rectangular shapes with sharp corners. The sharp rectangular shape points to an abrupt yielding behavior.[42] At the corners of the rectangle, a slight overshoot is visible in both the total stress and the elastic contribution to the stress (dashed line). The overshoot can be associated with the stretching of attractive droplet–droplet bonds under applied strain.[43] Due to such stretching, the stress within the emulsion increased momentarily and as the strain changed further, the bonds between the droplets were broken. Once the bonds were broken due to strain, the emulsion droplets started to flow as shown by the flat stress response with increasing strain. The structure breakdown indicates that the emulsion droplets in the presence of protein particles interact with each other mediated by the protein particles. The adhesive protein particles through van der Waals and hydrophobic interactions make the droplets "stick" to each other.[43,44] Therefore, pea protein stabilized emulsions with protein particles form a yielding, plastic-like material.

To confirm whether protein particles were solely responsible or if pH had an effect on the material response, emulsions were prepared at pH 3 after the removal of the protein particles. The rheological and microstructural properties of the jammed emulsions stabilized by pea proteins after removal of protein particles are shown in **Figure 6**.

The confocal image of jammed emulsion at pH 3 after removal of protein particles is shown in Figure 6c. It shows that the protein molecules were still able to produce stable jammed oil droplets. However, the interstitial space seems to be void of proteins, which confirms the protein particles being successfully removed.

The strain sweep of the emulsion at pH 3 prepared without protein particles is shown in Figure 6a. The graph shows G'
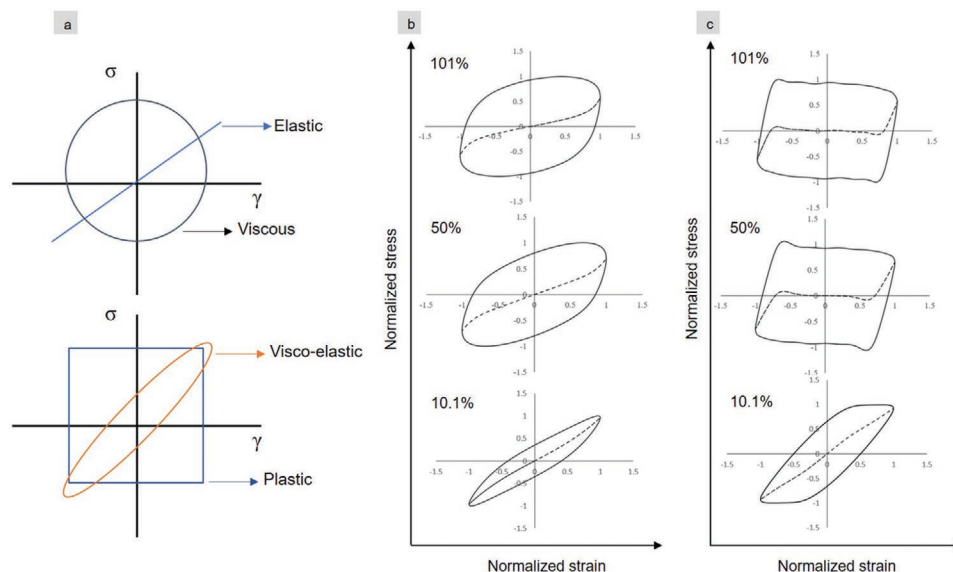
Figure 5. a) Reference Lissajous curves showing the basic shapes of standard material responses for reference and b) Lissajous curves of 70 wt% oil emulsions with pea protein molecules and c) Lissajous curves of 70 wt% oil emulsions with pea protein particles. As a function of increasing strain amplitude (10.1%, 50%, 101%) at constant frequency of 6.28 rad s⁻¹ at 20 °C with stress versus strain normalized by maximum stress and maximum strain, respectively.

ADVANCED
SCIENCE NEWS
www.advancedsciencenews.com

ADVANCED
FUNCTIONAL
MATERIALS
www.afm-journal.de

(filled circle) and G″ (unfilled circle) as a function of strain amplitude. As seen from the figure, G′ values were slightly higher than G″ at strain values below 20%. Above 20% the G″ was higher and the emulsion showed predominantly viscous behavior. The emulsions without particles at pH 3, had lower moduli values compared to emulsions that contained particles at the same pH value (Figure 2b, black curves). This behavior of the jammed emulsion at pH 3 in the absence of protein particles was similar to the jammed emulsion formed at pH 7, showing a clear effect of the protein particles on the rheological properties.[32]

Figure 6b shows Lissajous plots of jammed emulsion stabilized with pea proteins at pH 3, with (red) and without protein particles (black) as a function of different strain amplitudes. The shapes of the loops of the emulsions without protein particles at pH 3 is similar to that of jammed emulsions without protein particles at pH 7 (Figure 4b).

The shapes of the loops clearly showed that the emulsions without protein particles at pH 3 have a different microstructure compared to the emulsions with protein particles at pH 3 (red loops). When particles were not present, at 10% strain, the emulsion displayed a nonlinear viscoelastic response with mild strain hardening near the maximum strain, similar to the pH 7 emulsions. Moreover, when protein particles were not present, at 50% and 100% strains, the shapes of the curves were rounded rhomboids, whereas the presence of protein particles

resulted in sharp rectangular responses (yielding, plastic-like). Also, the overshoot in stress at the corners when particles were present is not seen when particles were absent.

Even though the mass fraction of proteins in the emulsions is much less compared to oil droplets (≈1:100), the particles are vital for creating plastic-like emulsions. The mechanism of microstructure formation stems from the presence of protein particles between oil droplets, as shown in **Figure 7**. The protein particles themselves are formed by protein–protein attractive hydrophobic and van der Waals forces.[21] Therefore, the protein particles create adhesive droplet–droplet interaction by "sticking" with interface-bound protein molecules through hydrophobic and van der Waals interactions. The droplet–droplet adhesion results in soft solid material with a plastic-like response.[45] Without protein particles, the oil droplets are simply jammed and do not form a printable material. An overview of the tested conditionas and results are provided in **Table 1**.

The ability to produce a 3D printable material using pea protein stabilized emulsions opens avenues for utilizing plant protein-based edible materials for specialized foods without the need for any additional cross-linking agent. For instance, pea protein-based emulsions could deliver hydrophobic molecules through encapsulation for special dietary needs and therapeutic foods.[10,46] By controlling the shape and fill density of the printed structure, encapsulation and release of molecules, and the sensorial attributes of the material can be modified.[47] Therefore,
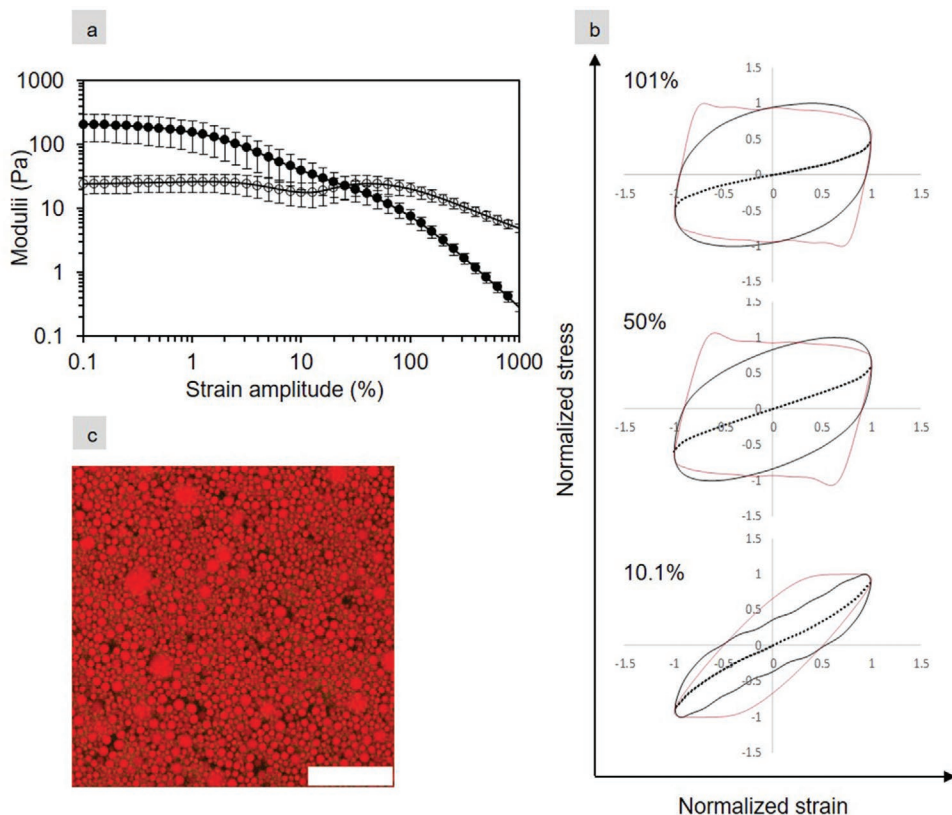
Figure 6. a) Elastic (G′: filled symbols) and loss modulus (G″: unfilled symbols) of 70 wt% oil emulsions (black) made at pH 3 after removal of protein particles by centrifugation plotted as a function of strain amplitude and b) Lissajous curves of 70 wt% emulsions after removal of protein particles (black), with stress versus strain normalized by maximum stress and strain, respectively. The Lissajous plots of 70 wt% emulsions at pH 3 with pea protein particles are given for reference (red). c) Confocal image of the emulsion showing the microstructure (scale bar: 50 μm).
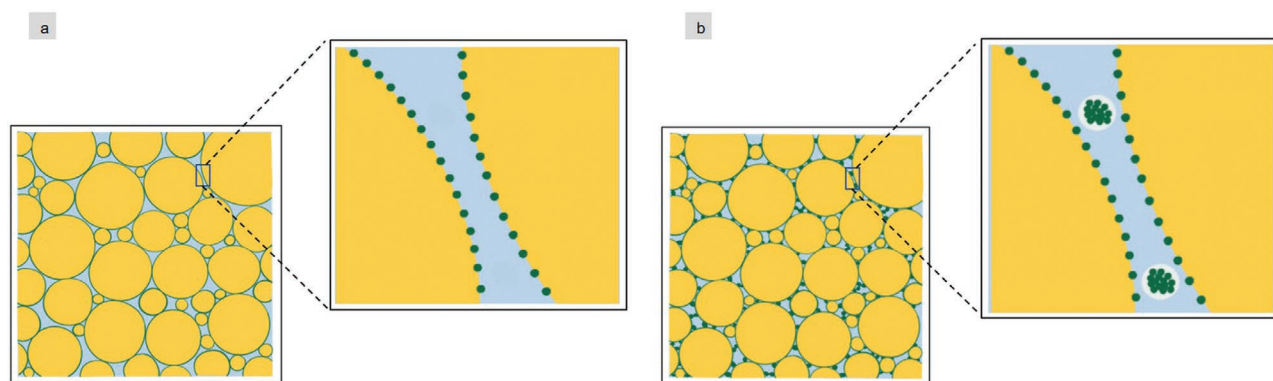
Figure 7. Graphical depiction of emulsion microstructure a) without protein particles showing oil droplets in contact with each other and b) with protein particles associating with the close packed oil droplets creating droplet–droplet interaction through weak adhesive forces.

plant protein-based materials could play a vital role in specialized foods. Beyond food, we envision that the printable material could even be used as sacrificial template for production of tissue analogues for instance in structured cultured meat research.

We created a 3D printable material by simply changing the pH of jammed emulsions stabilized by pea proteins and extruding it at room temperature. However, using nozzles of micrometer scale or use of elevated temperatures might affect the stability of emulsion droplets and thereby the stability of the printed material. Further studies on these aspects would be necessary.

3. Conclusion

3D printable materials should flow when applying an external force to get them through a nozzle and should be able to self-stand after printing. In this research, we successfully designed such an edible 3D printable material based on a jammed emulsion using the pH-dependent self-assembling property of pea proteins. The emulsions formed without protein particles (pH 7) were viscoelastic soft solids with only weak droplet–droplet interactions. Whereas emulsions formed in the presence of

protein particles (pH 3) behaved like elastoplastic material, with relatively strong adhesive droplet–droplet interaction. The protein particles through hydrophobic and van der Waals forces "stick" the droplets together. The printability of the two emulsions was tested using a 3D printer at room temperature. Emulsions without particles were not able to retain the printed structure, while the emulsions with protein particles were extruded were able to retain the printed structures for over 48 h. Therefore, using the self-assembled adhesive protein particles in a jammed emulsion, we designed a 3D printable material. The use of self-assembled adhesive pea protein particles is an attractive method to form edible 3D printable materials since proteins form an integral part of edible systems. This is the first time a simple pH driven technique is applied to create 3D printable edible emulsions structures based on plant proteins. Our method also eliminates additional pre and/or post-treatments used to stabilize the printed structures.[5] Therefore, our research opens up possibilities to employ accessible molecules such as pea proteins (plant proteins) to design edible printed emulsion structures. We envision more plant proteins would be explored as biopolymers to produce printable materials both for specialized foods and for biocompatible applications such as scaffolding.

Table 1. Summary table with the emulsion samples tested and the results of their rheological response and photograph of 3D printed structures.

Emulsion sample	Protein particles	Rheological property	3D printed structure
70 wt% oil-pH 7	No	Jammed emulsion-gel	
70 wt% oil-pH 3	Yes	Plastic material	
70 wt% oil-pH 3 without protein particles	No	Jammed emulsion-gel	N.A
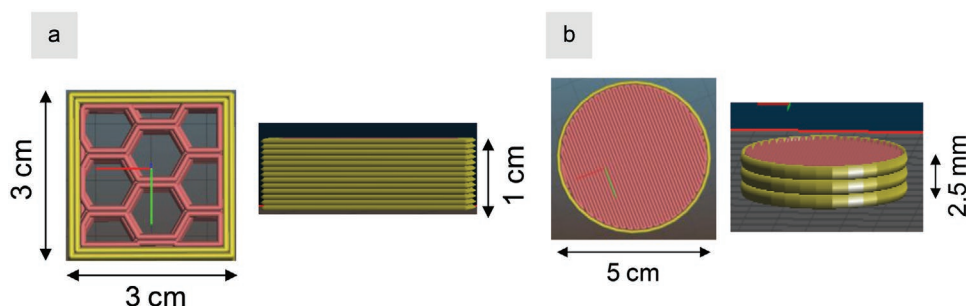
Figure 8. Model 3D printing structures generated and fed into the 3D printer. a) Honeycomb structure used to visually test the printability of the emulsions with dimensions (3 cm * 3 cm * 1 cm—*l*w*h*). b) Cylindrical shape printed to test the rheology of the emulsion postprinting with dimensions (Dia: 5 cm and *h*: 2.5 mm).

4. Experimental Section

Materials: Whole yellow field peas (*Pisum sativum L*) were obtained from Alimex BV (Sint Kruis, The Netherlands). Sodium Hydroxide, hydrochloric acid (analytical grade), sodium dodecyl sulphate (SDS) reagent, fluorescent dyes Nile red, and Fast Green were all obtained from Sigma-Aldrich (Zwijndrecht, The Netherlands). Whatmann cellulose thimbles were obtained from VWR (Amsterdam, The Netherlands).

Methods: Purification of Pea Proteins: Pea proteins were extracted from whole yellow peas by alkaline extraction and isoelectric point precipitation, which is commonly reported in literature.[48,49] In brief, pea seeds were dry milled into a coarse flour in a coffee blender (IKA, Staufen, Germany). The flour was then soaked in water at 1:10 (w:w) solids to water ratio. The pH was adjusted to pH 8 with a 0.5 M NaOH solution under constant stirring. After 2 h of soaking, the slurry was blended in a kitchen blender at maximum speed for 2 min. The resultant slurry was centrifuged at 10 000 g for 30 min to precipitate solids. Further, the protein-rich supernatant was separated, and the proteins were precipitated at a pH of 4.8 with a 0.5 M HCl solution. The solution was allowed to stand for 1 h and the precipitate was collected by centrifugation at 10 000 g for 30 min. The precipitate was diluted (1:10 w/w) with ultrapure water and pH was neutralized (pH 7). The solution was further freeze-dried, and the obtained powder was termed simply as pea protein. The protein powder was stored in the freezer (−18 °C) for further use.

Oil-in-Water Emulsion Preparation: Oil-in-water emulsions were prepared using pea protein dispersions as an aqueous phase. 70.0 wt% rapeseed oil and 30.0 wt% of protein dispersions were used. The final protein content of the emulsion was standardized to 1.4 wt% for 70 wt% oil emulsion by adjusting the protein content in the dispersion. The pH of the protein dispersion was changed to pH 3 or pH 7 using 0.5 M HCl or 0.5 M NaOH, respectively. The protein dispersion was then stirred for 3 h under magnetic stirring. The dispersion was then sheared for 15 s at 6000 rpm in an IKA (Ultra-Turrax, IKA, Staufen, Germany) to ensure homogeneous dispersion of proteins. Further, rapeseed oil was added slowly, and the mixture was sheared for another 60 s at 10 000 rpm to produce a coarse emulsion. The formed coarse emulsion was further homogenized by passing through a GEA (Niro Soavi NS 1001 L, Parma, Italy) high-pressure homogenizer at a homogenization pressure of 650 bars. The obtained final emulsion was allowed to equilibrate 3 h before any measurement was performed. The emulsions were called pea protein emulsions and were made in duplicates.

Emulsions were also prepared using pea protein solution (supernatant after removal of particles). In brief, pea protein dispersions were prepared as explained above. Then the dispersion was ultracentrifugated at 320 000 g for 45 min at 20 °C using a Beckman-Coulter L60 (Beckman-Coulter Nederland B.V, Woerden, The Netherlands) ultracentrifuge in 40 mL glass tubes. The clear supernatants were carefully collected by pouring them onto a beaker. The collected solution was called protein molecules solution. Emulsions were prepared as described above with this solution.

Droplet Size Measurement: The individual droplet size of the emulsions was measured using laser diffraction in Bettersizer (Bettersize Instruments Ltd., Hamburg, Germany). The samples were dispensed using a hydro dispenser and the droplet size was represented in volume mean diameter. To measure individual droplet sizes, the emulsions were treated with a 1.0 wt% SDS solution. The addition of SDS breaks droplet aggregation driven by protein interaction, so the size of individual oil droplets could be measured in this manner.[50] An equal volume of (1 mL) of emulsion and 1.0 wt% SDS solution was mixed and the size was immediately measured using a refractive index of 1.47.

Rheological Measurement: The rheological properties of protein dispersion and emulsions at pH 7 and pH 3 were measured at 20 °C using an Anton Paar 302 rheometer. The supplier software Rheocompass S1.25 was used to analyze and obtain raw data for all the measurements.

Emulsions were analyzed using oscillatory rheological measurements in a cone-plate set up with a cone diameter of 50 mm and cone angle of 4° (gap truncation of 0.49 mm). Before measurements, emulsions were allowed to equilibrate at room temperature for at least 1 h. The emulsions were then loaded onto the rheometer and the upper plate was lowered to the required gap. The emulsion was allowed to equilibrate for 5 min before the measurement was started. First, emulsions were tested for their linear viscoelastic regime using a strain amplitude sweep at a constant frequency of 6.2 rad s^{-1} (≈1 Hz). An amplitude where the modulus did not depend on strain value was chosen for further tests. Then a sequence of tests was performed starting with a frequency sweep test using a constant strain determined from the strain sweep experiment.

A fresh sample of the emulsion was used to probe the large amplitude oscillatory shear rheology (LAOS) experiment. The emulsion sample was loaded in the same manner and a strain sweep ranging from 0.1% strain up to 1000% strain at a constant frequency of 6.2 rad s^{-1} was performed. The raw waveforms collected during the sweep were analyzed using the MITlaos software, which was kindly provided as open source (MITlaos V2.1, freeware distributed from MITlaos@mit.edu). Lissajous–Bowditch curves were plotted of stress versus strain and stress versus strain rate. The shapes of these Lissajous curves provide essential microstructural information about the materials. For more information of the shapes, please refer to the Supporting Information.

To test the rheological behavior of the emulsion after 3D printing, the emulsions were first 3D printed in a cylindrical shape as described in the "3D Printing Emulsions" section below. To test the printed material, a 50 mm diameter plate–plate geometry was used. A serrated top plate was used to avoid any slip from the printed structure. A gap size of 2.5 mm was used. The 3D printed structures were carefully placed on the rheometer geometry and a frequency sweep was performed in a similar manner to the emulsions before 3D printing.

Confocal Laser Scanning Microscopy (CLSM): The emulsions were imaged using a CLSM with the aid of fluorescent dyes to visualize the microstructure. In brief, about 1 mL of the emulsion was mixed with 7 µL of Nile red and 7 µL of Fast green FCF in an eppendorf tube. The

tubes were sealed and allowed to mix for 15 min. Afterward, ≈30 µL of the sample was deposited on a microscopy slide and mounted on the confocal table. A Leica SP8 confocal microscope fitted with a 63× water immersion lens and white light laser was used to image the samples. Nile red stained the oil phase and was excited at 488 nm and the emission was captured between 500 and 600 nm. Rhodamine B which stained proteins was excited at 566 nm and the emission was captured between 570 and 670 nm. The images were captured in a sequential manner using Leica imaging software.

3D Printing of Emulsions: The emulsions were also 3D printed using a byFlow (Eindhoven, The Netherlands) commercial 3D printer. A cube geometry design of length 30 mm, width 30 mm, and height 10 mm was fed to the printer. A honeycomb fill of 20% infill density was set. The emulsions were extruded through a nozzle of size 1200 µm. The printing was conducted at a speed of 10 mm s^{-1}. In total, 13 layers were printed one on top of each other. The reference design for the printed structure is shown in **Figure 8**a.

To test the effect of 3D printing on the material, rheology of the emulsions after 3D printing were also measured. Same printing settings as described above were used. The freshly prepared emulsions were 3D printed on a soft surface in a dense cylinder shape with a radius of 5 cm and height of 2.5 mm. A 100% infill density in a rectilinear pattern was used. The reason for 3D printing a cylinder to measure rheology was to fit the material properly within a plate–plate geometry. Accurate filling (fitting) of the sample is essential to accurately measure the rheological property. The reference image of the cylindrical structure to be printed is shown in Figure 8b.

Supporting Information

Supporting Information is available from the Wiley Online Library or from the author.

Conflict of Interest

The authors declare no conflict of interest.

Data Availability Statement

Research data are not shared.

[1] M. R. Sommer, L. Alison, C. Minas, E. Tervoort, P. A. Rühs, A. R. Studart, *Soft Matter* **2017**, *13*, 1794.
[2] C. B. Highley, K. H. Song, A. C. Daly, J. A. Burdick, *Adv. Sci.* **2019**, *6*, 1801076.
[3] K. Vithani, A. Goyanes, V. Jannin, A. W. Basit, S. Gaisford, B. J. Boyd, *Pharm. Res.* **2019**, *36*, 1.
[4] X. Li, X. Xu, L. Song, A. Bi, C. Wu, Y. Ma, M. Du, B. Zhu, *ACS Appl. Mater. Interfaces* **2020**, *12*, 45493.
[5] C. He, M. Zhang, Z. Fang, *Crit. Rev. Food Sci. Nutr.* **2020**, *60*, 2379.
[6] S. Moon, J. Q. Kim, B. Q. Kim, J. Chae, S. Q. Choi, *Chem. Mater.* **2020**, *32*, 4838.
[7] S. Huan, R. Ajdary, L. Bai, V. Klar, O. J. Rojas, *Biomacromolecules* **2019**, *20*, 635.
[8] F. Yang, M. Zhang, B. Bhandari, *Crit. Rev. Food Sci. Nutr.* **2017**, *57*, 3145.
[9] H. Jiang, L. Zheng, Y. Zou, Z. Tong, S. Han, S. Wang, *Crit. Rev. Food Sci. Nutr.* **2019**, *59*, 2335.
[10] J. I. Lipton, M. Cutler, F. Nigl, D. Cohen, H. Lipson, *Trends Food Sci. Technol.* **2015**, *43*, 114.
[11] J. Y. Zhang, J. K. Pandya, D. J. McClements, J. Lu, A. J. Kinchla, *Crit. Rev. Food Sci. Nutr.* **2021**, 1.
[12] J. Sun, W. Zhou, L. Yan, D. Huang, L. Lin, *J. Food Eng.* **2018**, *220*, 1.
[13] A. Derossi, R. Caporizzi, D. Azzollini, C. Severini, *J. Food Eng.* **2018**, *220*, 65.
[14] T. Yang, Y. Hu, C. Wang, B. P. Binks, *ACS Appl. Mater. Interfaces* **2017**, *9*, 22950.
[15] Y. Liu, W. Zhang, K. Wang, Y. Bao, J. Mac Regenstein, P. Zhou, *Food Bioprocess Technol.* **2019**, *12*, 1980.
[16] J. Poore, T. Nemecek, *Science* **2018**, *360*, 987.
[17] A. C. Y. Lam, A. Can Karaca, R. T. Tyler, M. T. Nickerson, *Food Rev. Int.* **2018**, *34*, 126.
[18] T. G. Burger, Y. Zhang, *Trends Food Sci. Technol.* **2019**, *86*, 25.
[19] M. Chen, J. Lu, F. Liu, J. Nsor-Atindana, F. Xu, H. D. Goff, J. Ma, F. Zhong, *Food Hydrocolloids* **2019**, *88*, 247.
[20] H. N. Liang, C. H. Tang, *Food Hydrocolloids* **2013**, *33*, 309.
[21] S. Sridharan, M. B. J. Meinders, J. H. Bitter, C. V. Nikiforidis, *Langmuir* **2020**, *36*, 12221.
[22] A. K. Stone, A. Karalash, R. T. Tyler, T. D. Warkentin, M. T. Nickerson, *Food Res. Int.* **2015**, *76*, 31.
[23] K. J. Klemmer, L. Waldner, A. Stone, N. H. Low, M. T. Nickerson, *Food Chem.* **2012**, *130*, 710.
[24] K. Shevkani, N. Singh, A. Kaur, J. C. Rana, *Food Hydrocolloids* **2015**, *43*, 679.
[25] K. W. Desmond, E. R. Weeks, *Phys. Rev. E: Stat., Nonlinear, Soft Matter Phys.* **2014**, *90*, 022204.
[26] H. S. Kim, T. G. Mason, *Adv. Colloid Interface Sci.* **2017**, *247*, 397.
[27] D. Bonn, M. M. Denn, L. Berthier, T. Divoux, S. Manneville, *Rev. Mod. Phys.* **2017**, *89*, 035005.
[28] Y. Hemar, D. S. Horne, *Langmuir* **2000**, *16*, 3050.
[29] M. Hermes, P. S. Clegg, *Soft Matter* **2013**, *9*, 7568.
[30] M. C. Rogers, K. Chen, M. J. Pagenkopp, T. G. Mason, S. Narayanan, J. L. Harden, R. L. Leheny, *Phys. Rev. Mater.* **2018**, *2*.
[31] H. G. Sim, K. H. Ahn, S. J. Lee, *J. Non-netonian Fluid Mech.* **2003**, *112*, 237.
[32] K. N. Pham, G. Petekidis, D. Vlassopoulos, S. U. Egelhaaf, W. C. K. Poon, P. N. Pusey, *J. Rheol.* **2008**, *52*, 649.
[33] G. L. Hunter, E. R. Weeks, *Rep. Prog. Phys.* **2012**, *75*.
[34] S. S. Datta, D. D. Gerrard, T. S. Rhodes, T. G. Mason, D. A. Weitz, *Phys. Rev. E: Stat., Nonlinear, Soft Matter Phys.* **2011**, *84*, 3.
[35] C. Pellet, M. Cloitre, *Soft Matter* **2016**, *12*, 3710.
[36] V. Trappe, V. Prasad, L. Cipelletti, P. N. Segre, D. A. Weitz, *Nature* **2001**, *411*, 772.
[37] H. Liang, C. Tang, *LWT–Food Sci. Technol.* **2014**, *58*, 463.
[38] T. G. Mason, J. Bibette, D. A. Weitz, *Phys. Rev. Lett.* **1995**, *75*, 2051.
[39] E. D. Knowlton, D. J. Pine, L. Cipelletti, *Soft Matter* **2014**, *10*, 6931.
[40] R. H. Ewoldt, G. H. McKinley, A. E. Hosoi, *J. Rheol.* **2007**, *52*, 1427.

[41] K. Hyun, J. G. Nam, M. Wilhellm, K. H. Ahn, S. J. Lee, *Rheol. Acta* **2006**, *45*, 239.

[42] F. K. G. Schreuders, L. M. C. Sagis, I. Bodnár, P. Erni, R. M. Boom, A. J. van der Goot, *Food Hydrocolloids* **2021**, *110*.

[43] K. Hyun, J. G. Nam, M. Wilhelm, K. H. Ahn, S. J. Lee, *Korea-Australia Rheol. J.* **2003**, *15*, 97.

[44] K. Hyun, S. H. Kim, K. H. Ahn, S. J. Lee, *J. Non-netonian Fluid Mech.* **2002**, *107*, 51.

[45] A. Nesterenko, A. Drelich, H. Lu, D. Clausse, I. Pezron, *Colloids Surf., A* **2014**, *457*, 49.

[46] Y. K. Suppiramaniam, A. Thangarasu, A. Wilson, J. A. Moses, A. Chinnaswamy, *LWT–Food Sci. Technol.* **2021**, *146*, 111461.

[47] L. Zhao, M. Zhang, B. Chitrakar, B. Adhikari, *Crit. Rev. Food Sci. Nutr.* **2020**, 1.

[48] A. C. Karaca, N. Low, M. Nickerson, *Food Res. Int.* **2011**, *44*, 2742.

[49] J. I. Boye, S. Aksay, S. Roufik, S. Ribéreau, M. Mondor, E. Farnworth, S. H. Rajamohamed, *Food Res. Int.* **2010**, *43*, 414.

[50] N. Tangsuphoom, J. N. Coupland, *Food Hydrocolloids* **2008**, *22*, 1233.